

# Systemic and Specific Delivery of Small Interfering RNAs to the Liver Mediated by Apolipoprotein A-I

Soo In Kim<sup>1</sup>, Duckhyang Shin<sup>1</sup>, Tae Hyun Choi<sup>2</sup>, Jong Chan Lee<sup>2</sup>, Gi-Jeong Cheon<sup>2</sup>, Ki-Yong Kim<sup>3</sup>, Mahnhoon Park<sup>1</sup> and Meehyein Kim<sup>1</sup>

<sup>1</sup>Immunology and Virology Group, Mogam Biotechnology Research Institute, Yongin-si, South Korea; <sup>2</sup>Emergency Medical Team and Nuclear Medicine Laboratory, Korea Institute of Radiological and Medical Sciences, Seoul, South Korea; <sup>3</sup>Protein Research Laboratory, Green Cross Corporation, Yongin-si, South Korea

Tissue-targeted delivery of small interfering RNA (siRNA) must be achieved before RNA interference (RNAi) technology can be used in practical therapeutic approaches. In this study, the potential of apolipoprotein A-I (apo A-I) for the systemic delivery of nucleic acids to the liver is demonstrated using real-time *in vivo* imaging. As a proof of concept, synthetic siRNAs against hepatitis B virus (HBV) were formulated into complexes of apo A-I and 1,2-dioleoyl-3-trimethylammonium-propane (DOTAP)/cholesterol (DTC-Apo) and injected intravenously (IV) into a mouse model carrying replicating HBV. We show that administration of these nanoparticles can significantly reduce viral protein expression by receptor-mediated endocytosis. The advantages of the apo A-I-mediated siRNA delivery method are its liver specificity, its effectiveness at low doses ( $\leq 2$  mg/kg) in only a single treatment, and its persistent antiviral effect up to 8 days. The liver-targeted gene silencing was also shown by *in vivo* images, in which bioluminescent signals emitted from the liver were efficiently reduced after IV administration of luciferase-specific siRNA and DTC-Apo lipoplex. Thus, our unique approach to siRNA delivery creates a foundation for the development of a new class of promising therapeutics against hepatitis viruses or hepatocyte genes related to tumor growth.

Received 10 October 2006; accepted 11 March 2007; published online 17 April 2007. doi:10.1038/sj.mt.6300168

## INTRODUCTION

RNA interference (RNAi) is a gene silencing process induced by 21–23-nucleotide RNA duplexes called small interfering RNAs (siRNAs) and resulting in sequence-specific messenger RNA degradation post-transcriptionally in the cellular cytoplasmic region.<sup>1,2</sup> For the therapeutic application of siRNA, diverse approaches have been attempted to develop efficient delivery methods on the basis of clinically viable and acceptable administration strategies using viral vectors,<sup>3</sup> non-viral complexes,<sup>4–7</sup> or

antibody–protamine fusion proteins.<sup>8</sup> In particular, the systemic delivery of stable nucleic acid lipid particle-encapsulated<sup>5,9</sup> or cholesterol-conjugated<sup>10</sup> siRNAs has validated the *in vivo* RNAi effects against endogenous or viral hepatic RNAs in mice and non-human primates and has also led to the promise of their use in a clinical setting. However, improved technologies to enable liver-targeted delivery of siRNAs using non-viral vehicles that can transfer RNA molecules safely, efficiently, and selectively to the target organ via systemic routes is still a challenge.

In a recent report, recombinant high-density lipoprotein (HDL) was used as a carrier to deliver a lipophilic anti-tumor drug into human hepatocellular carcinoma cells *in vitro* but not *in vivo*, by taking advantage of the hydrophobic cholesterol ester-loading properties of HDL.<sup>11</sup> Taken together, these findings suggested that apolipoprotein A-I (apo A-I), which is a protein component of HDL that guides the transport of cholesterol from cells of the arterial wall to the liver and steroidogenic organs,<sup>12</sup> is conceptually applicable to liver targeting of nucleic acids or other, non-nucleic acid drugs. Most of all, apo A-I as a targeting moiety has noticeable advantages: it is predominantly taken up by the liver via the cell-surface receptor SR-BI (for mouse) or Cla-1 (for human), its recycling or catabolic pathway has been well characterized, and the protein itself is an endogenous product, so it should not be detrimental to humans and it should not trigger immunological side effects in clinical applications.

Accordingly, this study was conducted to determine the feasibility and effectiveness of using native apo A-I for the delivery of liposomes containing synthetic siRNA to the liver via systemic routes *in vivo*. Here, we show that apo A-I can be formulated onto the surface of the lipid bilayer of a representative cationic liposome, 1,2-dioleoyl-3-trimethylammonium-propane (DOTAP)/cholesterol, and that it can facilitate the hepatocyte-specific release of the nucleic acid payload via receptor-mediated endocytosis. Using a mouse model carrying actively replicating hepatitis B virus (HBV) or expressing a bioluminescence protein in the liver, we show that the subsequent inhibition of target protein expression can be monitored via the secreted viral protein levels in serum and by *in vivo* imaging analysis of the

**Correspondence:** Meehyein Kim, Immunology and Virology Group, Mogam Biotechnology Research Institute, 341, Bojeong-dong, Giheung-gu, Yongin-si, Kyonggi-do 449-913, South Korea. E-mail: mkim@mogam.re.kr

expression of the bioluminescence protein in the mouse whole body, respectively.

## RESULTS AND DISCUSSION

### Apo A-I characterization

Human apo A-I (28 kd) was highly purified according to an established protocol<sup>13</sup> from normal healthy adult blood not infected with viral pathogens such as HBV, hepatitis C virus, or human immunodeficiency virus (**Figure 1a**), and its identity was also verified by western blot analysis with an apo A-I-specific polyclonal antibody (data not shown). Our preliminary interest was to determine whether the purified human apo A-I retained the native structure required for recognition by the cell-surface receptor SR-BI and targeting to hepatic cells *in vivo*. Thus, we labeled it with an infrared fluorescence dye before injecting it into mice via the tail vein with normal pressure. With a real-time imaging system, apo A-I biodistribution in whole, live mice was assessed at several time points (**Figure 1b**). The imaging analysis revealed that systemically administered apo A-I can be specifically delivered to and stably maintained in the liver for at least 6 hours. Fluorescent signals observed in the bladder are likely to represent elimination of the protein from the body by urination, resulting in irregular fluorescent intensities in each bladder (data not shown). Kinetic analysis of photon intensities in the liver showed that the uptake yield of the input apo A-I was maximal at approximately 45% within 150 minutes after treatment (**Figure 1c**). Next, we determined anatomically whether labeled apo A-I accumulated in the liver not in other internal organs. Thus, mice were killed, and selective organs (heart, lung, spleen, kidney, adrenal gland, ovary, and liver) were collected and examined for apo A-I uptake 24 hours after systemic injection of fluorescence-labeled apo A-I or fluorescent dye only. As shown in **Figure 1d**, substantial fluorescent signals associated

with apo A-I distribution were detected in the liver but not in thoracic or other internal organs, except for the kidney, which is known to be another site for the renal clearance of free or HDL-associated apo A-I after catabolic processes.<sup>14,15</sup> In contrast, the infrared dye used as a control material was not internalized stably in any organ. In addition, this liver-targeted delivery of apo A-I protein through blood circulation was confirmed by a microPET imaging study using <sup>124</sup>I-labeled apo A-I (data not shown), indicating its ability to penetrate deep hepatic tissue. Taken together, these data demonstrate that purified free apo A-I maintained its native conformation required for cell-surface receptor recognition and catabolic circulation *in vivo*, suggesting that it might be applicable as a potent liver targeting moiety in feasibility studies for gene therapy.

### Hepatocyte-specific gene delivery *in vitro*

To investigate whether apo A-I can guide hydrophilic nucleic acids to hepatic cells by a mechanism of receptor-mediated endocytosis, we chose cationic liposomes composed of DOTAP and cholesterol (hereafter designated DTC) as carriers and characterized the gene-transfer properties of apo A-I-decorated DTC (hereafter designated DTC-Apo). Particle size analysis revealed that the average diameters of DTC and DTC-Apo encapsulating nucleic acids were approximately 200 and approximately 180 nm, respectively, indicating that these particles are homogeneously assembled and suitable for systemic administration (**Table 1**). Moreover, zeta potential values of both DTC and DTC-Apo particles were positive (approximately 40–50 mV). In previous reports, it was pointed out that assembly of negatively charged protein onto cationic liposomes can cause the net charge to shift from positive to negative and subsequently promote their gene-delivery efficiency. This appears to occur by alleviation of undesirable interactions

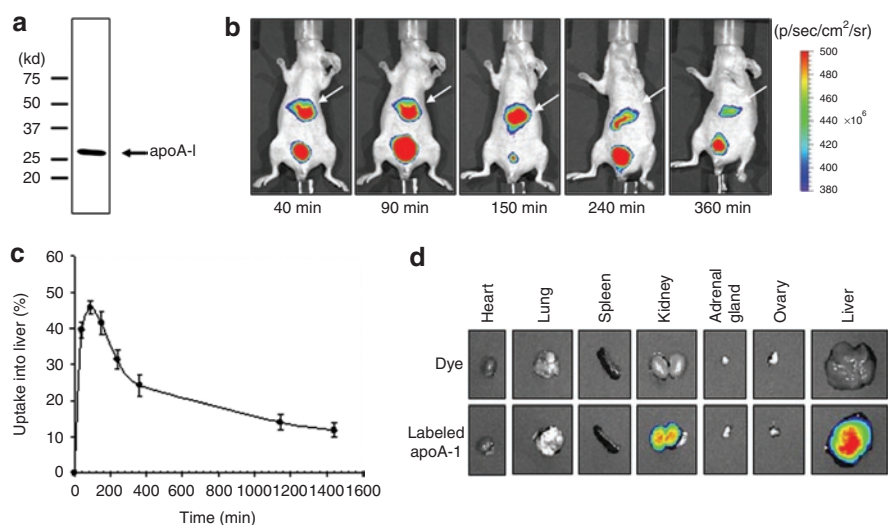


**Figure 1** Liver-targeted delivery of free apolipoprotein A-I (apo A-I). **(a)** Purified human apo A-I separated by 4–20% sodium dodecyl sulfate–polyacrylamide gel electrophoresis is indicated by an arrow on the right and the molecular weights of the marker proteins, in kilodaltons (kd), are shown on the left of the gel. **(b)** *In vivo* images of a representative live nude mouse intravenously injected with 200  $\mu$ g of apo A-I labeled with an infrared fluorescent dye at several times after injection. Systemically administered apo A-I migrates to the liver (indicated with white arrows) before being eliminated from the body by urination. **(c)** Percentage uptake rate of the labeled protein in the liver at different time points ( $n = 4$ ). The total fluorescence intensity of the injected solution was measured before injection. **(d)** Mice were exsanguinated and selective organs were isolated from the body to measure apo A-I biodistribution anatomically.

**Table 1** Size and zeta potential measurements of cationic nanoparticles<sup>a</sup>

Formulation	Size (nm)	ζ pot (mV)
DTC	176.5 ± 1.4	53.3 ± 4.0
DTC with DNA <sup>b</sup>	205.5 ± 4.2	42.7 ± 1.8
DTC with siRNA <sup>c</sup>	196.0 ± 1.8	44.6 ± 2.2
DTC-Apo	147.9 ± 2.8	49.5 ± 6.3
DTC-Apo with DNA <sup>b,d</sup>	179.5 ± 3.4	38.6 ± 4.0
DTC-Apo with siRNA <sup>c,d</sup>	177.1 ± 1.4	39.1 ± 2.8

Abbreviations: ζ pot, zeta potential; DTC-Apo, apo A-I–decorated DOTAP/cholesterol; si RNA, small interfering RNA.

<sup>a</sup>Sizes are given as diameters in nanometers; all values are noted as means ± SD. *n* = 3. Particles are resuspended in 5% dextrose solution. <sup>b</sup>DNA is pRL-CMV. <sup>c</sup>siRNA is a non-specific control siRNA. <sup>d</sup>DOTAP/cholesterol:apoA-I:nucleic acids = 10:1:1 (wt/wt/wt).

between lipoplexes and unknown serum components not in a receptor-mediated manner.<sup>16,17</sup> However, in our study, the similar zeta potentials of both preparation sets indicate that the anionic apo A-I scarcely influences the positive net charge of the lipoplex. In other words, it means that improvement of gene-transfer efficiency mediated by apo A-I is not associated with the “charge shielding” effect.

We examined changes in the transfection ability of DTC by apo A-I and compared gene delivery efficiencies of DTC and DTC-Apo in hepatic and non-hepatic cells *in vitro*. In this experiment, it was observed that loading of apo A-I onto DTC resulted in an increase in the transfection yield, specifically in human hepatocyte-derived cells, HepG2 and Huh7, but not in non-hepatic cells, B16F10 (Figure 2a–c). The improved transfection efficiency by apo A-I was correlated with the expression levels of its cell-surface receptor SR-BI and Cla-1 (Figure 2d). Moreover, in competition assays, both SR-BI-specific and apo A-I-specific antibodies decreased the transfection efficiency of DTC-Apo, but not of DTC, into HepG2 cells in a dose-dependent manner (Supplementary Figure S1). These results provide direct support for our hypothesis that apo A-I can mediate gene transport into hepatic cells through interactions with its cell-surface receptors.

### Liver-specific gene delivery *in vivo*

Further to validate the preferential delivery potency of apo A-I to hepatocytes *in vivo*, we prepared DTC-Apo particles containing the pRL-CMV plasmid (named DTC-Apo/RLuc), which expresses the *Renilla* luciferase gene. Apo A-I was labeled with <sup>125</sup>I (named DTC-Apo\*/RLuc) to facilitate the systemic and sensitive detection of its migration route, and biodistribution of the particles was monitored by whole-body imaging at different time points after intravenous (IV) injection. As shown in Figure 3a, the gamma camera photograph (the left picture) at 120 minutes revealed that DTC-Apo\*/RLuc complexes accumulated in hepatic tissue. Mouse organ distribution was determined from an X-ray photograph (the right picture). As mentioned, the isotope signals in the bladder indicate that after separation of the protein ligand component from the lipoplex particles, it could be eliminated from the body by urination, similar to free apo A-I (see also Figure 1b). Furthermore, the property of liver-oriented migration of the apo A-I–coupled lipoplex was also evaluated by insertion of <sup>125</sup>I-*N*-succinimidyl-3-(4-hydroxyphenyl)propionate

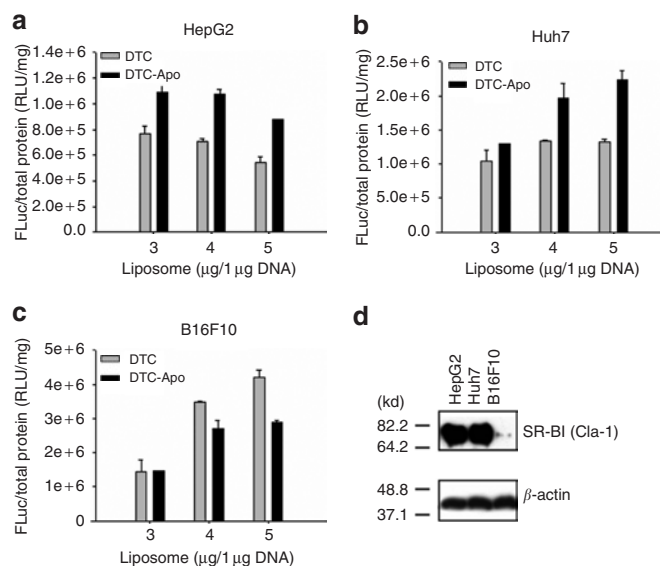


**Figure 2** Hepatocyte-specific gene delivery by apolipoprotein A-I–decorated DOTAP/cholesterol (DTC-Apo) liposomes *in vitro*. DTC or DTC-Apo liposomes (3–5 μg) containing 1 μg pEGFP-Luc DNA were transfected into human liver cell lines, (a) HepG2 and (b) Huh7, or into a mouse melanoma cell line, (c) B16F10. At day 2 after transfection, cell lysates were harvested to measure luciferase expression levels. All transfection experiments were performed in 12-well plates in triplicate. (d) The expression levels of the apo A-I receptor, SR-BI and Cla-1, for the different cell lines were assessed by western blot analysis. β-actin served as an internal loading control.

(<sup>125</sup>I-SHPP)–linked dioleoyl phosphatidylethanolamine (DOPE) into the cationic liposome (named DTC\*). To compare the quantity of DTC\* and DTC\*-Apo liposomes taken up by the organs, we killed mice 3, 6, and 24 hours after systemic administration and collected the organs as well as blood for radioactive counting using a gamma counter (Figure 3b; Supplementary Table S1). As shown in Figure 3b, which represents quantitative biodistribution at 6 hours after injection, the accumulation level of DTC\*-Apo was enhanced in the liver by approximately threefold compared with that of simple DTC\*. This definitively shows that the apo A-I in DTC-Apo liposomes plays a key role in delivering nanoparticles to the liver selectively and efficiently. To obtain critical and direct evidence that DTC-Apo particles can subsequently release their nucleic acid components into the cytoplasm or nucleus of hepatocytes *in vivo*, we injected mice IV with unlabeled DTC-Apo/RLuc or DTC/RLuc particles and measured the bioluminescence intensities in tissue homogenates from heart, lung, kidney, and liver by the luciferase assay (Figure 3c). Before measuring luciferase levels, we confirmed that there were neither distinctive body weight differences nor organ weight variations among individuals. Consistent with liver-specific accumulation of isotope-labeled DTC-Apo vehicle (Figure 3b), luminescence signals were particularly concentrated in the mouse liver 24 hours after IV injection of DTC-Apo/RLuc, with a range of 6,700–50,300 relative luciferase units per 1 mg of total protein. In contrast, in mice treated with DTC/RLuc, luciferase signals were detected strongly in the lung and kidney but only modestly in the liver, and there was only basal luciferase expression in the naked DNA-treated or 5% dextrose mock-treated groups. Although DTC-Apo/RLuc administration showed the high

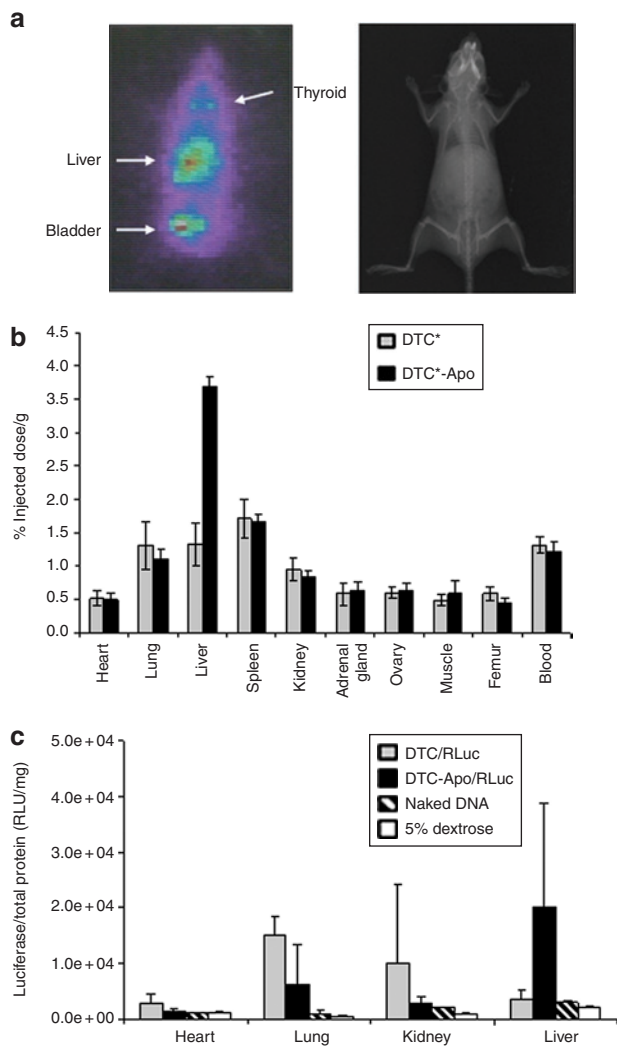


**Figure 3** Apolipoprotein A-I (apo A-I)-mediated migration into the liver of cationic liposomes. **(a)** The apo A-I component in DOTAP/cholesterol (DTC)-Apo complexes encapsulating the phRL-CMV plasmid was labeled with  $^{131}\text{I}$  and administered to mice by standard intravenous (IV) injection ( $200\ \mu\text{Ci}$  per mouse). Whole-body images for radioiodine signals were captured using a gamma camera after injection (left). Organs with detectable radioactive signals are indicated with arrows at 120 minutes. Mouse organ distribution was determined from an X-ray photograph (right). **(b)** Organ distribution of DTC\* and DTC\*-Apo was measured. After IV administration of  $15\ \mu\text{Ci}$  of DTC\* and DTC\*-Apo, organs and blood ( $n = 4$ ) were collected for monitoring biodistribution of particles. The radioactivity was counted using a gamma counter in triplicate and expressed as a percentage of the injected dose per gram of tissue at 6 hours. **(c)** Liver-specific gene delivery by the DTC-Apo vehicle. Mice ( $n = 3$ ) were systemically administered with a mock control (5% dextrose), naked DNA, DTC/RLuc, or DTC-Apo/RLuc at a dose of  $40\ \mu\text{g}$  phRL-CMV per mouse and killed 1 day after administration. Luciferase levels were measured in tissue homogenates from heart, lung, kidney, and liver and then expressed as relative luciferase units (RLUs) per mg total protein. Values represent mean  $\pm$  SD.

SD of the mean efficiency of the reporter gene delivery in the liver, these luciferase expression levels were significantly increased when compared with simple DTC/RLuc treatment ( $P < 0.05$ ). Our results provide fundamental evidence and a rationale for the use of apo A-I in the development of liver-directed non-viral gene delivery methods that accompany receptor-mediated endocytosis.

## RNAi effects against HBV

To examine the therapeutic activity of DTC-Apo-encapsulated siRNA, we chose HBV as a target for RNAi-mediated inhibition because it replicates exclusively in the liver. Quantitative estimation of *in vivo* RNAi efficacy of the DTC-Apo-formulated HBV X-specific siRNA (DTC-Apo/siHBV) was facilitated by a mouse model of acute HBV infection. We generated this model system by hydrodynamic injection of an HBV-replicating plasmid, pCpGHBV-MBRI, into mice. Compared with the mother clone, pHBV-MBRI,<sup>18</sup> the backbone-modified pCpGHBV-MBRI plasmid was designed to express viral antigens at elevated levels over longer periods of time *in vivo* (data not shown), as this plasmid backbone does not induce non-specific inflammatory responses in mammalian hosts. The relative expression levels of apo A-I receptor, SR-BI, were measured by western blot analysis before and after hydrodynamic injection of pCpGHBV-MBRI into adult C57BL/6 mice. As shown in **Figure 4a**, transient HBV replication in liver did not affect SR-BI expression levels, demonstrating that the concept of apo A-I-mediated siRNA delivery is applicable in this acute HBV mouse model. Eight hours after hydrodynamic injection of  $10\ \mu\text{g}$  pCpGHBV-MBRI into mice, they were treated again with an IV injection of  $2\ \text{mg/kg}$  ( $40\ \mu\text{g}$  siRNA per mouse) DTC/siRNA, DTC-Apo/siRNA, naked siRNA, or a 5% dextrose mock control. At different times, serum HBV surface antigen, one of the major viral structural proteins, was measured by enzyme-linked immunosorbent assay (**Figure 4b**). Notably, a significant reduction in serum HBV surface antigen was observed in mice administered DTC-Apo/siHBV particles in a single dose, as shown by average inhibitions of 65.1% ( $P = 0.014$ ), 63.4% ( $P = 0.047$ ), 74.9% ( $P = 0.015$ ), and 72.8% ( $P = 0.034$ ) on days 2, 4, 6, and 8 after injection, respectively, relative to the matched DTC-Apo/siCont group. Although simple DTC/siHBV particles reduced viral antigen expression in some individuals, with a maximum reduction of 43% relative to DTC/siCont as observed in a previous report,<sup>6</sup> this group showed wide variations among individual animals and failed to yield statistical evidence for an RNAi effect. We further tested the dose-dependent activity of DTC-Apo/siHBV. Mice with acute HBV replication were treated with 0.5, 1, or  $2\ \text{mg/kg}$  doses of HBV-targeted siRNA, and the serum viral antigen levels were monitored at day 2 after injection. As shown in **Figure 4c**, the reduction in viral antigen expression reached saturation at a dose of  $1\ \text{mg/kg}$  siRNA, and the results were statistically significant ( $P < 0.01$ ) in both groups treated with 1 and  $2\ \text{mg/kg}$  siHBV relative to the control treated with  $2\ \text{mg/kg}$  siRNA. In addition, the enhanced siRNA delivery to the liver mediated by the targeting moiety apo A-I was validated again in another acute HBV mouse model system using pHBV-MBRI with an additional HBx-specific sequence, siHBV-3, which was selected in our previous study<sup>18</sup> (sequence in **Supplementary Table S2; Supplementary Figure S2**). Our *in vivo* data indicate that apo A-I assembled on cationic lipids promotes the hepatic tissue-specific delivery of siRNA and that a single IV treatment of a mature formulation containing anti-HBV siRNAs leads to potent gene silencing effects on viral replication *in vivo*.

## RNAi in the liver

Although evidence in this study demonstrates DTC-Apo/siRNA-mediated silencing of hepatitis viral replication, questions about

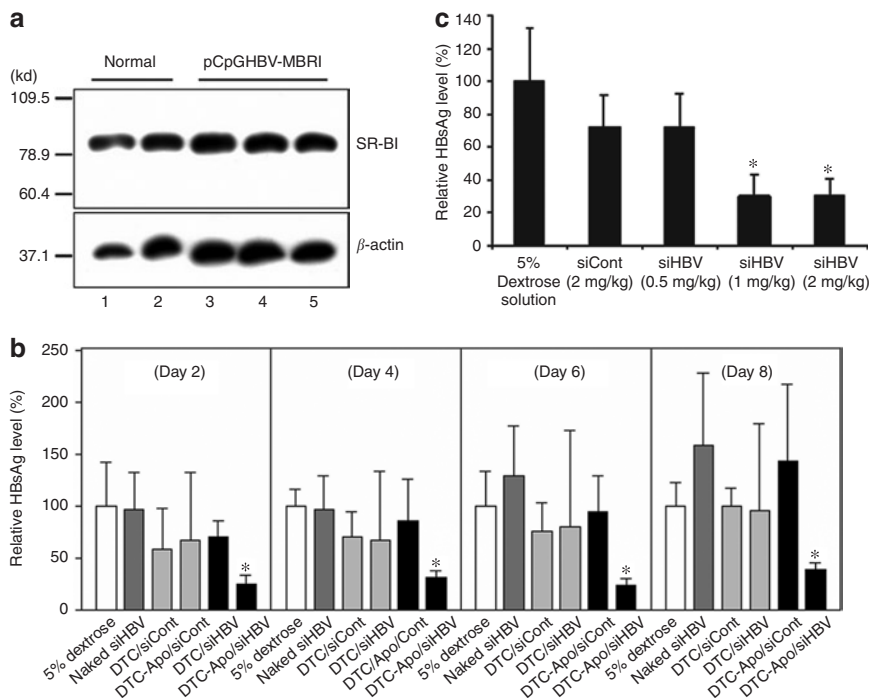


**Figure 4** Therapeutic silencing of viral protein levels after a single treatment with apolipoprotein A-I–decorated DOTAP/cholesterol (DTC-Apo)–encapsulated hepatitis B virus (HBV)–specific small interfering RNA (siRNA) in an HBV mouse model. **(a)** The protein expression levels of the apo A-I receptor were estimated in mouse liver specimens. Total liver homogenates of normal mice (lanes 1 and 2) and mice hydrodynamically injected with 10  $\mu$ g of pCpGHBV-MBRI (lanes 3–5) were probed for SR-BI (upper) and  $\beta$ -actin as a loading control (lower). **(b)** Female C57BL/6 mice were hydrodynamically injected with 10  $\mu$ g of pCpGHBV-MBRI. Eight hours later, naked HBV X-specific siRNA (siHBV), DTC/siCont, DTC/siHBV, DTC-Apo/siCont, or DTC-Apo/siHBV was intravenously administered at a dose of 2 mg/kg, and blood serum was harvested at days 2, 4, 6, and 8 after injection. Relative levels of secreted HBV surface antigen (HBsAg) were determined by enzyme-linked immunosorbent assay (ELISA) and normalized against the average level of the 5% dextrose control. Values represent mean  $\pm$  SD ( $n = 4$ ). \* $P < 0.05$  compared with the matched control group. **(c)** Dose-dependent RNA interference effect of the systemically administered DTC-Apo/siHBV in the same *in vivo* mouse model of HBV replication. DTC-Apo-encapsulated HBV-specific siRNA or irrelevant control siRNA was injected into HBV-replicating mice at doses of 0.5, 1, and 2 mg/kg by standard tail vein injection. At day 2 after injection, serum HBsAg levels were measured by ELISA and expressed as mean  $\pm$  SD ( $n = 4$ ). DTC-Apo/siHBV reduced viral protein expression at 1 and 2 mg/kg doses significantly. \* $P < 0.01$  compared with the control siRNA group.

whether this RNAi machinery occurs selectively and mainly in the hepatic tissue remained to be addressed. We therefore prepared another mouse model for *in vivo* imaging by hydrodynamic injection of a target plasmid, pEGFP<sub>Luc</sub>, which expresses the firefly luciferase gene and facilitates *in vivo* image analysis. One day after target injection of pEGFP<sub>Luc</sub>, DTC-Apo/siRNAs were administered IV into Balb/c female mice, as described above. When DTC-Apo/siCont or naked siLuc was injected, mice showed no inhibition of luciferase expression, and when DTC/siLuc was injected, mice showed a slight but not significant gene silencing effect (Figure 5; Supplementary Figure S3). In contrast, systemic injection of a complex of DTC-Apo/siLuc (1 and 2 mg/kg siRNA per mouse) exhibited a dramatic reduction in luciferase activity (approximately 70% in Figure 5 and 95% in Supplementary Figure S3, respectively) as early as day 1 after treatment compared with the DTC-Apo/siCont group.

As a toxicology study, we characterized the short-term safety profile associated with systemic DTC-Apo/siRNA administration. For serological and histological analysis, serum and organs were collected from mice at day 1, 2, or 3 after IV injection for each preparation. Two main serum aminotransferase (alanine aminotransferase and aspartate aminotransferase) levels, as well as serum albumin, bilirubin, and alkaline phosphatase levels,

were measured (Supplementary Tables S3 and S4). In parallel, a histopathological analysis of liver, lung, heart, kidney, and spleen was performed (Supplementary Figure S4). These results were reviewed by board-certified pathologists. From these clinical assessments of the serum alanine aminotransferase and aspartate aminotransferase levels and organ histopathology, none of the preparations led to significant toxic effects on liver or other organs of animals. However, it could not be excluded that the presence of additive apo A-I protein (40  $\mu$ g per mouse), even though its injection dose was insignificant, influenced cholesterol metabolism or induced an undesirable balance of lipoproteins. Therefore, serum cholesterol and triglyceride levels were also estimated (Supplementary Tables S5 and S6). Notably, neither DTC-Apo/siRNA nor any of its components had an effect on the serum levels of total cholesterol, HDL or low-density lipoprotein cholesterol, or triglycerides. Taken together, these results show that liver is the selective target for DTC-Apo/siRNA particles administered systemically and that siRNA released from the nanoparticles can trigger the RNAi pathway, without inducing any enzymatic abnormalities or pathological damage in normal liver function.

To the best of our knowledge, this is the first report to demonstrate the liver-targeted delivery of therapeutic siRNA via receptor-mediated endocytosis. Our findings suggest that DTC-Apo

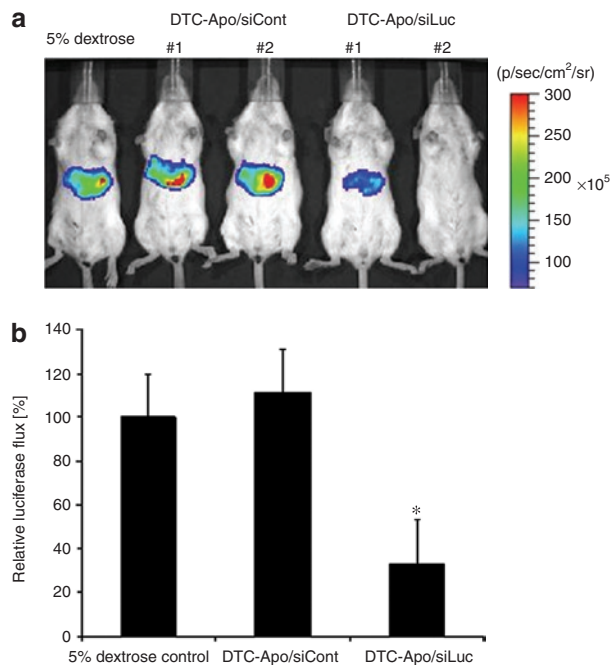


**Figure 5** *In vivo* images of inhibition of the luciferase gene expression by apolipoprotein A-I-decorated DOTAP/cholesterol (DTC-Apo)/siRNA duplexes targeting luciferase (siLuc). **(a)** Representative images of Balb/c mice that were hydrodynamically injected with  $10\mu\text{g}$  of the luciferase expression plasmid, pEGFP<sub>Luc</sub>, and, 1 day after target injection, intravenously treated with 1 mg/kg DTC-Apo/siCont or DTC-Apo/siLuc in 200  $\mu\text{l}$  of 5% dextrose solution. **(b)** Relative luciferase expression levels were measured by counting bioluminescence signals emitted from the liver of the mice. Data are from four individuals and expressed as means  $\pm$  SD. \* $P < 0.05$  compared with the control siRNA group.

nanoparticles, composed of apo A-I (the protein component of HDL) and cationic DTC liposomes, can be used to carry siRNA molecules to the animal liver selectively. As a proof of concept, we showed that DTC-Apo-formulated HBV-specific siRNA significantly diminished expression levels of viral surface protein in acute HBV infection models after treatment with a single dose. *In vivo* imaging also confirmed that this RNAi-based mechanism might be implicated in systemic siRNA delivery to the hepatic tissue. Importantly, our supplementary data indicate that (i) after assembly, the tertiary structure of apo A-I  $\alpha$ -helical domains that are critical for binding to SR-BI (or Cla-1)<sup>19,20</sup> remained nearly intact ( $\geq 77\%$ ) and were exposed on the lipid particle surface (Supplementary Figure S5) and (ii) the expression level of the cell-surface receptor for apo A-I was maintained in cell lines or mouse livers with transient HBV replication compared with respective control groups, or increased approximately fourfold in persistently HBV-replicating cells *in vitro* (Figure 4a; Supplementary Figure S6). These points decisively addressed the potency of apo A-I as a therapeutic target moiety, especially against viral hepatitis.

Currently, there are several reports concerning non-specific interferon and/or immunostimulatory responses to unmodified synthetic siRNA-cationic liposome complexes that activate the Toll-like receptor signals of immune cells.<sup>21–23</sup> It has also been suggested that activation of the immune system by liposome-formulated siRNAs and associated toxicities could be triggered

in a nucleotide sequence-dependent manner.<sup>24</sup> We observed that DTC-Apo/siRNAs (DTC-Apo/siCont, DTC-Apo/siHBV, DTC-Apo/siHBV-3, and DTC-Apo/siLuc) stimulated interferon and inflammatory cytokines such as interferon- $\alpha$ , interferon- $\gamma$ , tumor necrosis factor- $\alpha$ , and interleukin-6 without sequence-specific differences and transiently within 6 hours after injection (data not shown). Notably, no changes were detected in mouse body weight or behavior, the histological cell morphology, or liver function after administration of DTC-Apo/siRNA at a maximum of 2 mg/kg dose (data not shown; Supplementary Figure S4; Supplementary Tables S3–6). In recent reports, it was elucidated that this undesirable immunostimulatory activity of liposome-siRNA complexes can be clearly eliminated by chemical modification of siRNAs,<sup>5,22,25</sup> which allow the siRNA to escape the Toll-like receptor-mediated response. Thus, our further studies are focusing on selection of chemically modified siRNAs suitable to the DTC-Apo-derived gene-delivery system to increase RNA stability as well as immuno-safety. This approach will be required before using siRNA in small-molecule drug strategies. Nevertheless, this study sufficiently shows that the use of an unstable, unmodified RNA in the DTC-Apo-formulated complex is able to yield significant, long-lasting (more than 8 days) silencing activity at low doses ( $\leq 2$  mg/kg), even after a single IV injection into an acute HBV-infected mouse model.

Here, we demonstrated the feasibility of a systemic and non-viral ligand-mediated RNAi gene therapy using endogenous protein apo A-I. This strategy allowed the effective delivery of siRNAs to the liver and release of nucleic acids into hepatic cells and, finally, reduced target gene expression. Thus, our unique and promising approach using DTC-Apo A-I-formulated siRNA nanoparticles may allow the development of a new class of therapeutics to down-regulate hepatitis viruses or endogenous genes involved in the growth of hepatocellular carcinomas.

## MATERIALS AND METHODS

**siRNAs.** All siRNAs used in these studies were purchased from Bioneer (Daejeon, South Korea). The sequences of the sense and antisense strands of the control, HBV-specific,<sup>18</sup> and firefly luciferase-specific<sup>1</sup> siRNAs are detailed in Supplementary Table S2. The double-stranded siRNAs were characterized by denaturing and non-denaturing polyacrylamide gel electrophoresis.

**Animal studies.** All animal studies were performed in accordance with the Guidelines for the Care and Use of Laboratory Animals prepared by the National Academy of Sciences.

**Plasmid DNA.** The plasmids pRL-CMV, encoding *Renilla* luciferase, and pEGFP<sub>Luc</sub>, encoding firefly luciferase, were purchased from Promega (Madison, WI) and Clontech (Palo Alto, CA), respectively. The HBV replication-competent plasmid, pCpGHBV-MBRI, was created by excision of the viral genome from the mother clone pHBV-MBRI<sup>18</sup> and re-ligation into *Spe*I- and *Xba*I-digested pCpG-mcs (InvivoGen, San Diego, CA) for the sensitive and extended expression of viral antigens in immunocompetent mice.

**In vivo imaging of free apo A-I biodistribution.** Human apo A-I protein was isolated from plasma fractions by cold ethanol precipitation as described previously.<sup>13</sup> After sodium dodecyl sulfate-polyacrylamide gel electrophoresis, apo A-I was characterized by Coomassie blue staining, and its identity was confirmed by western blot analysis using a goat

anti-human apo A-I antibody (Academy Biomedical Company, Houston, TX), which has cross-reactivity to mouse apo A-I, and a secondary antibody, rabbit anti-goat IgG-horseradish peroxidase (KPL, Gaithersburg, MD). The expression level of the apo A-I receptor, SR-BI or Cla-1, in mouse organs or cell lines was measured by western blot analysis using a rabbit anti-SR-BI antibody (Novus Biologicals, Littleton, CO) and a horseradish peroxidase-conjugated goat anti-rabbit IgG (KPL, Gaithersburg, MD). For *in vivo* imaging, the purified protein (0.6 mg) was labeled with an infrared dye using IRDye 800 CW *in vivo* imaging agents (LI-COR Biosciences, Lincoln, NE) according to the manufacturer's instructions and purified using a dextran desalting column (Pierce Biotechnology, Rockford, IL) to remove the unincorporated dye. Free infrared dye or labeled apo A-I (200 µg) with the same photon intensity was administered to 6–8-week-old female nude mice (Charles River Laboratories, Wilmington, MA) via tail vein injection. After 10 minutes of anesthesia with 2% isoflurane, each animal was placed in a supine position in a light-tight chamber, and whole-body images were obtained using the IVIS 200 imaging system and Living Image Software (Xenogen, Alameda, CA). At 24 hours after treatment with labeled apo A-I, mice were exsanguinated and perfused with saline. Organs (heart, lung, spleen, kidney, adrenal gland, ovary, and liver) were collected and examined for fluorescent image analysis using the IVIS 200 imaging system (Xenogen, Alameda, CA).

**Formulation of DTC-Apo and nucleic acids.** To prepare conventional cationic DTC liposomes, we mixed chloroform (Sigma, St. Louis, MO) solutions of lipids at the equimolar ratio of DOTAP (Avanti Polar Lipids, Alabaster, AL) and cholesterol (Sigma, St. Louis, MO).<sup>26,27</sup> After liposome assembly, the organic solvent was evaporated under a stream of N<sub>2</sub> gas. Vacuum desiccation for 2 hours ensured removal of the residual organic solvent. The dried film was hydrated in a 5% dextrose solution and then the liposomal suspension was sonicated using a bath sonicator. To formulate DTC-Apo, the DTC liposomes suspended in 5% dextrose solution were reassembled with A-I protein solution (at a ratio of 10:1 (wt/wt) DTC:protein) overnight at 4 °C. For *in vitro* treatment, 1 µg of plasmid DNA was mixed with 3–5 µg of DTC or DTC-Apo liposomes in 200 µl of Opti-MEM (Gibco BRL–Invitrogen, Life Technologies, Gaithersburg, MD), incubated at room temperature for 30 minutes, and then transfected into cells. In *in vivo* experiments of liver-specific gene delivery, 40 µg of siRNAs or plasmid DNA was mixed with 400 µg of the empty cationic liposomes in 200 µl of 5% dextrose solution and the mixture was incubated at room temperature for 30 minutes. Before *in vivo* administration and *in vitro* transfection, the formulated particles were characterized by measuring their size and charge using a Zetasizer 3000 apparatus (Malvern Instruments, Malvern, Worcestershire, UK).

**Cell culture studies.** HepG2, Huh7, and B16F10 cells were maintained in Dulbecco's modified Eagle's medium (Gibco, Life Technologies, Gaithersburg, MD) supplemented with 10% fetal bovine serum (Gibco, Life Technologies, Gaithersburg, MD). Cells were plated (2 × 10<sup>5</sup> cells/well) in 12-well plates and incubated overnight. One microgram of a reporter gene expression DNA, pEGFP-Luc (Clontech, Palo Alto, CA), encapsulated in increasing amounts of DTC or DTC-Apo (3–5 µg), was added to wells in triplicate. The medium was changed 4 hours later and cells were collected as lysates after 48 hours for the luciferase assay (Luciferase Assay System; Promega, Madison, WI).

**Labeling of DTC-Apo.** DTC-Apo liposomes (3 mg) were assembled with 0.3 mg of phRL-CMV (Promega, Madison, WI) and then the protein component was labeled with 0.6 mCi <sup>131</sup>I (The Korea Atomic Energy Research Institute, Daejeon, South Korea) by the chloramine-T method (named DTC-Apo\*/RLuc).<sup>28</sup> In parallel, the lipid component of DTC-Apo was also radiolabeled. In brief, Bolton–Hunter reagent (SHPP; Pierce, Rockland, IL) as a linker was labeled with <sup>131</sup>I according to a modified chloramine-T method (named <sup>131</sup>I-SHPP).<sup>28,29</sup> Empty cationic liposomes consisting of

DOTAP, cholesterol, and DOPE (Avanti Polar Lipids, Alabaster, AL) were prepared at a molar ratio of 50:30:20 DTC/DOPE (named DTC-DOPE), and then the DTC-DOPE was conjugated with <sup>131</sup>I-SHPP by incubation in pH 8.5 borate buffer for 3 hours on ice (named DTC\*). Unincorporated <sup>131</sup>I-SHPP was removed using a dextran desalting column (Pierce, Rockland, IL). DTC\* was mixed with apo A-I at a weight ratio of 10:1 DTC\*/apo A-I (named DTC\*-Apo) at 4 °C overnight.

**In vivo imaging of DTC-Apo biodistribution.** To monitor biodistribution of the complexed DTC-Apo\*/RLuc, we injected the purified lipoplex (200 µCi) IV into nude mice (Charles River Laboratories, Wilmington, MA) and monitored the radioactivity from the whole mouse using a gamma camera (Medical Imaging Electronics, Elk Grove Village, IL). In a second approach, complexes of DTC\* or DTC\*-Apo were IV injected into female C57BL/6 mice (15 µCi/head). Organs and blood (n = 4) were collected at 3, 6, and 24 hours after injection and their radioactivity was counted in triplicate using the <sup>131</sup>I channel of the multi-channel analyzer 1480 WIZARD (Wallac Perkin Elmer, CT). The radioactivity in each organ was expressed as a percentage of the injected dose per gram. In a third approach, to examine nucleic acid release by lipoplexes after systemic injection, we IV treated mice (n = 3 per group) with unlabelled DTC or DTC-Apo containing phRL-CMV (Promega, Madison, WI) and killed them the following day. Luciferase expression levels per total protein were measured in homogenate samples from heart, lung, kidney, and liver using a *Renilla* luciferase assay system (Promega, Madison, WI).

**Antiviral activity of DTC-Apo/siHBV in mice.** To assess the *in vivo* antiviral effect of DTC-Apo-formulated HBV-specific siRNAs (DTC-Apo/siHBV), we established an acute HBV-infected mouse model. In brief, 10 µg of a replication-competent plasmid, pCpGHBV-MBRI, was hydrodynamically injected into female C57BL/6 mice (Charles River Laboratories, Wilmington, MA) of 8–9 weeks of age weighing approximately 20 g.<sup>30</sup> After 8 hours, groups of four mice with replicating HBV in their livers were IV administered 10, 20, or 40 µg (*i.e.*, 0.5, 1, or 2 mg/kg) of siRNAs incorporated into the DTC or DTC-Apo liposomes at a constant ratio of 10:1 (wt/wt) liposome:siRNA. To monitor viral protein levels secreted into the blood, we collected serum on days 2, 4, 6, and 8 after DTC-Apo (or DTC)/siRNA injection and determined HBV surface antigen levels by enzyme-linked immunosorbent assay (DiaSorin, Stillwater, OK). The absorbance from normal mice was used as the background for this study.

**In vivo imaging of RNAi activity by DTC-Apo/siLuc.** To assess the RNAi effect visually in living animals, we prepared a luciferase-expressing mouse model by hydrodynamic injection with 10 µg of pEGFP-Luc plasmid (Clontech, Palo Alto, CA) into 6–7-week-old female Balb/c mice (Charles River Laboratories, Wilmington, MA). DTC-Apo/siCont or DTC-Apo/siLuc was injected at a dose of 1 mg/kg via the tail vein under normal pressure 1 day after target DNA injection. On subsequent days, mice were anesthetized with 2% isoflurane and intraperitoneally injected with 200 µl of 15 mg/ml D-luciferin (Molecular Imaging Products Company, Ann Arbor, MI) solution, according to the manufacturer's instructions. Ten minutes later, photon signals from whole bodies were quantified using the IVIS imaging system (Xenogen, Alameda, CA). In parallel with the *in vivo* imaging analysis, serum and organs (liver, lung, heart, kidney, and spleen) of mice treated with 5% dextrose (mock control), naked control siRNA, empty DTC, DTC-Apo liposomes, or DTC/siRNA or DTC-Apo/siRNA lipoplexes were harvested at day 1, 2, or 3 after injection. Necropsies and both histopathological and serological analyses were performed by board-certified pathologists at Green Cross Reference Laboratories (Yongin-si, Kyonggi-do, South Korea) to examine for toxicity.

**Statistical analysis.** Statistical analyses were performed using Student's *t*-test to measure statistical differences among groups. Data with *P* < 0.05 were considered to be statistically significant.

## ACKNOWLEDGMENTS

This work was supported by funds from Green Cross Corporation, South Korea.

## SUPPLEMENTARY MATERIAL

**Figure S1.** Cell-surface receptor-mediated gene delivery by DTC-Apo *in vitro*.

**Table S1.** Comparative study of liver-specific accumulation of <sup>131</sup>I-labeled lipid of DTC and DTC-Apo particles administered intravenously.

**Table S2.** Sense and antisense siRNA sequences used in these studies.

**Figure S2.** RNAi effects of DTC-Apo-encapsulated HBV-specific siRNAs in an HBV mouse model.

**Figure S3.** *In vivo* RNAi effects of DTC-Apo-encapsulated siRNAs directed against firefly luciferase mRNA.

**Table S3.** Total albumin, bilirubin, alkaline phosphatase, aspartate aminotransferase, and alanine aminotransferase levels in mouse serum after intravenous injection of any component or full particles of DTC-Apo/siRNA.

**Table S4.** Total albumin, bilirubin, alkaline phosphatase, aspartate aminotransferase, and alanine aminotransferase levels in mouse serum after intravenous injection of DTC-Apo/siRNA.

**Figure S4.** Histological sections from mouse organs.

**Table S5.** Cholesterol and triglyceride levels in mouse serum after intravenous injection of any components or full particles of DTC-Apo/siRNA.

**Table S6.** Cholesterol and triglyceride levels in mouse serum after intravenous injection of DTC-Apo/siRNA.

**Figure S5.** CD spectra of apo A-I protein.

**Figure S6.** Western blot analysis of Cla-1.

## REFERENCES

- Elbashir, SM, Harborth, J, Lendeckel, W, Yalcin, A, Weber, K and Tuschl, T (2001). Duplexes of 21-nucleotide RNAs mediate RNA interference in cultured mammalian cells. *Nature* **411**: 494–498.
- Hannon, GJ (2002). RNA interference. *Nature* **418**: 244–251.
- Wang, X, Skelley, L, Cade, R and Sun, Z (2006). AAV delivery of mineralocorticoid receptor shRNA prevents progression of cold-induced hypertension and attenuates renal damage. *Gene Ther* **13**: 1097–1103.
- Landen, CN Jr, Chavez-Reyes, A, Bucana, C, Schmandt, R, Deavers, MT, Lopez-Berestein, G *et al.* (2005). Therapeutic EphA2 gene targeting *in vivo* using neutral liposomal small interfering RNA delivery. *Cancer Res* **65**: 6910–6918.
- Morrissey, DV, Lockridge, JA, Shaw, L, Blanchard, K, Jensen, K, Breen, W *et al.* (2005). Potent and persistent *in vivo* anti-HBV activity of chemically modified siRNAs. *Nat Biotechnol* **23**: 1002–1007.
- Sorensen, DR, Leirdal, M and Sioud, M (2003). Gene silencing by systemic delivery of synthetic siRNAs in adult mice. *J Mol Biol* **327**: 761–766.
- Urban-Klein, B, Werth, S, Abuharbeid, S, Czubayko, F and Aigner, A (2005). RNAi-mediated gene-targeting through systemic application of polyethylenimine (PEI)-complexed siRNA *in vivo*. *Gene Ther* **12**: 461–466.
- Song, E, Zhu, P, Lee, SK, Chowdhury, D, Kussman, S, Dykxhoorn, DM *et al.* (2005). Antibody mediated *in vivo* delivery of small interfering RNAs via cell-surface receptors. *Nat Biotechnol* **23**: 709–717.
- Zimmermann, TS, Lee, AC, Akinc, A, Bramlage, B, Bumcrot, D, Fedoruk, MN *et al.* (2006). RNAi-mediated gene silencing in non-human primates. *Nature* **441**: 111–114.
- Soutschek, J, Akinc, A, Bramlage, B, Charisse, K, Constien, R, Donoghue, M *et al.* (2004). Therapeutic silencing of an endogenous gene by systemic administration of modified siRNAs. *Nature* **432**: 173–178.
- Lou, B, Liao, XL, Wu, MP, Cheng, PF, Yin, CY and Fei, Z (2005). High-density lipoprotein as a potential carrier for delivery of a lipophilic antitumoral drug into hepatoma cells. *World J Gastroenterol* **11**: 954–959.
- von Eckardstein, A, Nofer, JR and Assmann, G (2001). High density lipoproteins and arteriosclerosis. Role of cholesterol efflux and reverse cholesterol transport. *Arterioscler Thromb Vasc Biol* **21**: 13–27.
- Lerch, PG, Fortsch, V, Hodler, G and Bolli, R (1996). Production and characterization of a reconstituted high density lipoprotein for therapeutic applications. *Vox Sang* **71**: 155–164.
- Glass, C, Pittman, RC, Civen, M and Steinberg, D (1985). Uptake of high-density lipoprotein-associated apoprotein A-I and cholesterol esters by 16 tissues of the rat *in vivo* and by adrenal cells and hepatocytes *in vitro*. *J Biol Chem* **260**: 744–750.
- Webb, NR, Cai, L, Ziemba, KS, Yu, J, Kindy, MS, van der Westhuyzen, DR *et al.* (2002). The fate of HDL particles *in vivo* after SR-BI-mediated selective lipid uptake. *J Lipid Res* **43**: 1890–1898.
- Simoes, S, Pires, P, da Cruz, MT, Duzgunes, N and de Lima, MC (2003). Gene delivery by cationic liposome-DNA complexes containing transferrin or serum albumin. *Methods Enzymol* **373**: 369–383.
- Simoes, S, Slepishkin, V, Pires, P, Gaspar, R, Pedroso de Lima, MC and Duzgunes, N (2000). Human serum albumin enhances DNA transfection by lipoplexes and confers resistance to inhibition by serum. *Biochim Biophys Acta* **1463**: 459–469.
- Shin, D, Kim, SI, Kim, M and Park, M (2006). Efficient inhibition of hepatitis B virus replication by small interfering RNAs targeted to the viral X gene in mice. *Virus Res* **119**: 146–153.
- Vishnyakova, TG, Bocharov, AV, Baranova, IN, Chen, Z, Remaley, AT, Csako, G *et al.* (2003). Binding and internalization of lipopolysaccharide by Cla-1, a human orthologue of rodent scavenger receptor B1. *J Biol Chem* **278**: 22771–22780.
- Williams, DL, de La Llera-Moya, M, Thuahnai, ST, Lund-Katz, S, Connelly, MA, Azhar, S *et al.* (2000). Binding and cross-linking studies show that scavenger receptor B1 interacts with multiple sites in apolipoprotein A-I and identify the class A amphipathic alpha-helix as a recognition motif. *J Biol Chem* **275**: 18897–18904.
- Ma, Z, Li, J, He, F, Wilson, A, Pitt, B and Li, S (2005). Cationic lipids enhance siRNA-mediated interferon response in mice. *Biochem Biophys Res Commun* **330**: 755–759.
- Marques, JT and Williams, BR (2005). Activation of the mammalian immune system by siRNAs. *Nat Biotechnol* **23**: 1399–1405.
- Sioud, M and Sorensen, DR (2003). Cationic liposome-mediated delivery of siRNAs in adult mice. *Biochem Biophys Res Commun* **312**: 1220–1225.
- Judge, AD, Sood, V, Shaw, JR, Fang, D, McClintock, K and MacLachlan, I (2005). Sequence-dependent stimulation of the mammalian innate immune response by synthetic siRNA. *Nat Biotechnol* **23**: 457–462.
- Judge, AD, Bola, G, Lee, AC and MacLachlan, I (2006). Design of noninflammatory synthetic siRNA mediating potent gene silencing *in vivo*. *Mol Ther* **13**: 494–505.
- Kim, SI, Kim, KS, Kim, HS, Kim, DS, Jang, Y, Chung, KH *et al.* (2003). Inhibitory effect of the salmosin gene transferred by cationic liposomes on the progression of B16BL6 tumors. *Cancer Res* **63**: 6458–6462.
- Templeton, NS, Lasic, DD, Frederik, PM, Strey, HH, Roberts, DD and Pavlakis, GN (1997). Improved DNA: liposome complexes for increased systemic delivery and gene expression. *Nat Biotechnol* **15**: 647–652.
- Hunter, R (1970). Standardization of the chloramine-T method of protein iodination. *Proc Soc Exp Biol Med* **133**: 989–992.
- Bolton, AE and Hunter, WM (1973). The labelling of proteins to high specific radioactivities by conjugation to a <sup>125</sup>I-containing acylating agent. *Biochem J* **133**: 529–539.
- Liu, F, Song, Y and Liu, D (1999). Hydrodynamics-based transfection in animals by systemic administration of plasmid DNA. *Gene Ther* **6**: 1258–1266.